OAK RIDGE NATIONAL LABORATORY LIBRARIES
3 4456 0550935 8

ORNL-TM-5183

Cy 26

The Absolute Neutron Spectrum Emerging Through the Large Beam Collimator from the TSR-II Reactor at the Tower Shielding Facility

R. E. Maerker
F. J. Muckenthaler

[redacted]

OAK RIDGE NATIONAL LABORATORY
CENTRAL RESEARCH LIBRARY
DOCUMENT COLLECTION
LIBRARY LOAN COPY
DO NOT TRANSFER TO ANOTHER PERSON
If you wish someone else to see this
document, send in name with document
and the library will arrange a loan.

OAK RIDGE NATIONAL LABORATORY
OPERATED BY UNION CARBIDE CORPORATION • FOR THE U.S. ATOMIC ENERGY COMMISSION

Printed in the United States of America. Available from
the Energy Research and Development Administration,
Technical Information Center
P.O. Box 62, Oak Ridge, Tennessee 37830
Price: Printed Copy $5.00 ; Microfiche $2.25

This report was prepared as an account of work sponsored by the United States Government. Neither the United States nor the Energy Research and Development Administration, nor any of their employees, nor any of their contractors, subcontractors, or their employees, makes any warranty, express or implied, or assumes any legal liability or responsibility for the accuracy, completeness or usefulness of any information, apparatus, product or process disclosed, or represents that its use would not infringe privately owned rights.

ORNL-TM-5183
UC-79d

Contract No. W-7405-eng-26

Neutron Physics Division

THE ABSOLUTE NEUTRON SPECTRUM EMERGING THROUGH THE LARGE BEAM COLLIMATOR FROM THE TSR-II REACTOR AT THE TOWER SHIELDING FACILITY

R. E. Maerker and F. J. Muckenthaler

JANUARY 1976

NOTICE This document contains information of a preliminary nature and was prepared primarily for internal use at the Oak Ridge National Laboratory. It is subject to revision or correction and therefore does not represent a final report.

OAK RIDGE NATIONAL LABORATORY
Oak Ridge, Tennessee 37830
operated by
UNION CARBIDE CORPORATION
for the
U. S. ENERGY RESEARCH AND DEVELOPMENT ADMINISTRATION

OAK RIDGE NATIONAL LABORATORY LIBRARIES

3 4456 0550935 8

Abstract

The neutron spectral intensities in a 51-group structure together with the angular distributions in an 8-angle quadrature set are presented which describe the surface leakage from the hemispherical pressure vessel surrounding the TSR-II reactor at the Tower Shielding Facility. These data may be used as free-field source terms in the calculations of experiments performed using the large beam collimator, and were derived from many different measurements made at various positions in the beam that were used to normalize ANISN calculations of the pressure vessel leakage.

The geometry of the collimator arrangement to which the following data apply is shown in Fig. 1.

The neutron energy and angular distributions at any point on the surface of the hemispherical pressure vessel (for example, point A in Fig. 1) are presented in Table I. These distributions are derived from ANISN calculations of the pressure vessel leakage normalized to fit the detailed measurements of the neutron energy and spatial distributions in the free field.[1] The spectrum is presented in a 51-group structure, but it may be assumed to be smoothly varying and can thus be regrouped into any desired structure. Similar remarks apply to the angular distributions. Note that the entries in the table are integrated over the group interval, and are also expressed on an absolute watt basis.

[1] C. E. Clifford and F. J. Muckenthaler, "A Determination of the Neutron Energy and Spatial Distributions of the Neutron Beam from the TSR-II in the Large Beam Shield," ORNL-TM-4868, 1976.

This is the result of successfully determining experimentally the ratio between "monitor watts" and fission watts, by measurement of the temperature rise in the reactor cooling water, so that all data in this report are expressed in terms of "fission" or "heating" watts. This had not yet been done when an earlier report[2] describing the free-field from the 15¼-in. collimator was written. Thus the intensities in ORNL-TM-4010 should be multiplied by 0.658 to put them on the same basis as in the present report; i.e., per fission watt.

The units of the angular flux are neutrons/cm^2/min/fission watt/unit weight. To convert to angular current leaking the hemisphere in units of neutrons/cm^2/min/fission watt/steradian, each entry should be multiplied by the appropriate value of $\cos\theta_n/4\pi$, where θ_n is the angle between the normal to the surface and the direction of the angular flux.

The angular distributions given in Table I are not readily useable in a DOT calculation because they are defined with respect to a hemispherical surface, which is not yet a viable option in DOT. They must be transformed to angular distributions with respect to a plane surface, to take advantage of an existing option in DOT that uses a boundary disc source. This transformation can easily be effected by the following equation:

$$\phi_{g_p}(Z,R,\eta,\mu) = \phi_{g_h}(R_s,\cos\theta_n)\ \cos\theta_n/|\eta|,\ 0 \leq \cos\theta_n \leq 1 \quad ,$$

---

[2] R. E. Maerker and F. J. Muckenthaler, "The Absolute Neutron Spectrum Emerging Through a 15¼-in. Collimator from the TSR-II Reactor at the Tower Shielding Facility," ORNL-TM-4010, 1972.

where ϕ_{g_p} = group angular flux on a plane located a centerline distance Z from the reactor center in the cylindrical coordinate directions defined by η and μ, and at a distance R from the center of the plane, and ϕ_{g_h} = group angular flux on the hemisphere of radius R_s = 48.5775 cm interpolated from Table I at the angle $\cos\theta_n$.

The relationship between the variables η, μ, and $\cos\theta_n$ is

$$\cos\theta_n = \frac{R^2 + Z^2 - R_s^2 - A^2}{2R_s A}$$

where $A \equiv |\eta|\ Z + \mu R - \sqrt{R_s^2 + (|\eta|\ Z + \mu R)^2 - (R^2 + Z^2)}, \quad -1 \leq \mu \leq 1$.

A logical choice for the location of this disc source is at Z = 55.514 cm; i.e., on the plane defined by the inside concrete surface of the large beam collimator. The disc source should be written as an interior boundary source so that reflection from a cylindrical representation of the pressure vessel and water on the reactor side of the source plane as well as from the walls of the concrete collimator is included when transport through a shielding configuration is to be calculated. (Fig. 2).

The source transformation from a hemisphere to a disc involves only uncollided transport from hemisphere to disc. The effect of neutrons that leak the pressure vessel and are scattered by the stainless steel and water shield surrounding much of the pressure vessel to points on the disc plane is not considered in the transformation. This enhancement is included, however, in the adjustment of the source terms appearing in Table I.

A listing of the code effecting the transformation is presented in the Appendix. Also appearing in the Appendix is an example of angular and radial meshes used at ORNL to specify the disc source, together with the angular fluxes for the first group that appear on the interior boundary source tape. As a further check, the source description as presented in the output of a DOT calculation using this source tape is also displayed, for groups 1 through 49.

The source terms presented in Table I have been normalized so that the transformed planar interior boundary source, when used with the collimator geometry of Fig. 2 in a DOT calculation, gives rise to free field distant centerline fluxes and fluxes across the collimator exit plane that agree to within $\pm$ 15% of absolute measured values.[1] If the hemispherical source description were used directly with the values given in Table I and the effects of increased reflection included from a stainless steel and water region surrounding much of the pressure vessel, free field fluxes would be overcalculated by about 15%. Thus, if the hemispherical source geometry together with reflection geometry around the sides of the pressure vessel were actually incorporated into a calculation, the values appearing in Table I should be multiplied by 0.85.

Relative to the 15¼-in. collimator described in ORNL-TM-4010, the large beam collimator produces a centerline current above 0.9 MeV incident on the front face of a shield of about 35 times more, and a surface integrated current of about 190 times more, on an equal wattage basis. Since the maximum power available for the large beam collimator is 1 MW compared to 100 kW for the 15¼-in. collimator, the overall maximum increases in the incident current are 350 and 1900, respectively.

This increase in intensity is of course at the expense of a less well-defined beam. Neutron scattering from the concrete collimator and the stainless-steel-water shield in the large beam shield accounts for ∿ 25% of the flux above 0.9 MeV at the collimator exit, whereas for the 15¼-in. collimator, the effects of collimator scattering in this energy region were negligible.

ORNL-DWG 75-15295

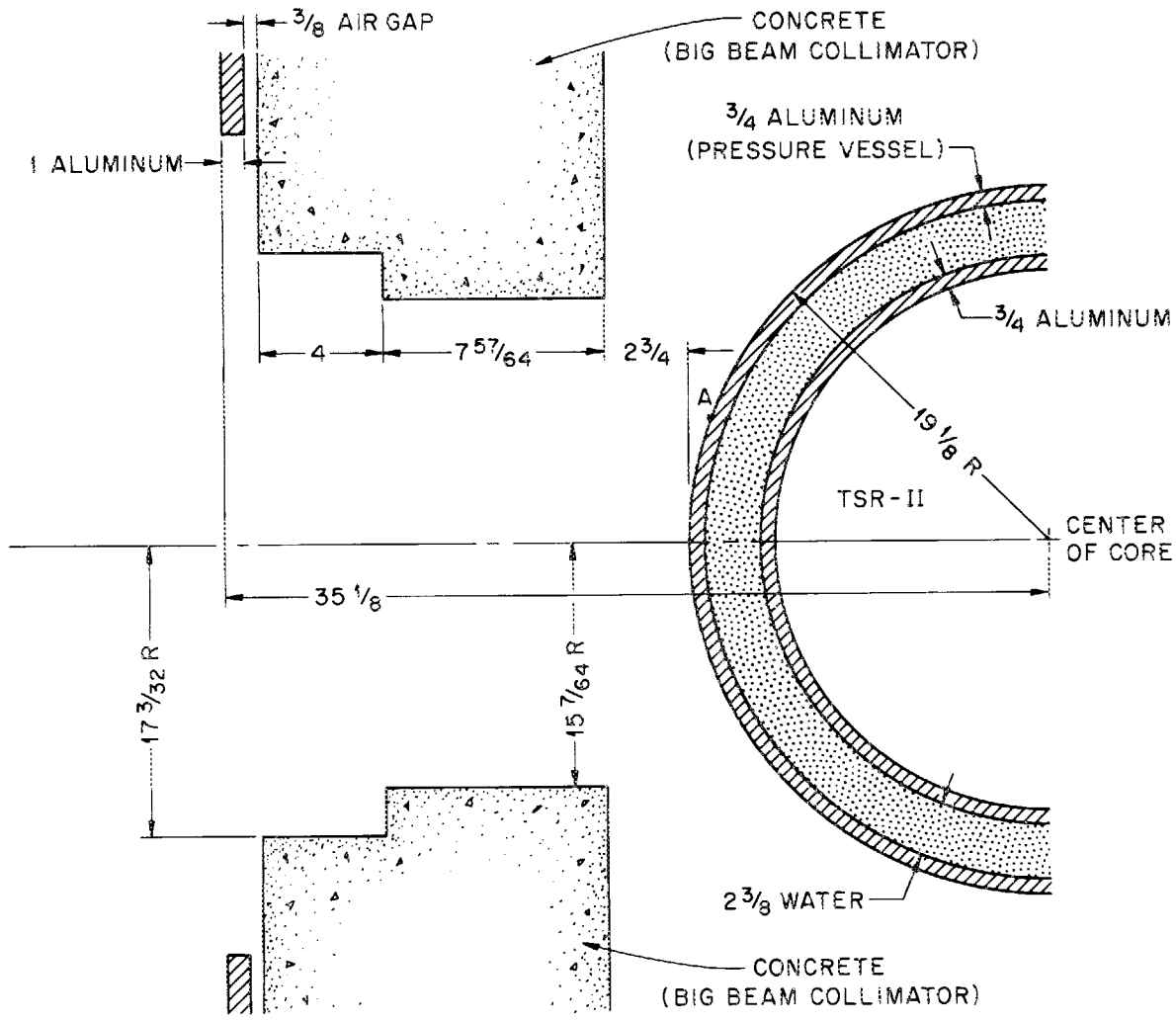

DIMENSIONS ARE IN INCHES (NOT TO SCALE)

Fig. 1. Simplified Top View of the Large Beam Collimator. A Stainless Steel-Water Region (not pictured) Surrounds the Pressure Vessel at all Points not Exposed to the Collimator

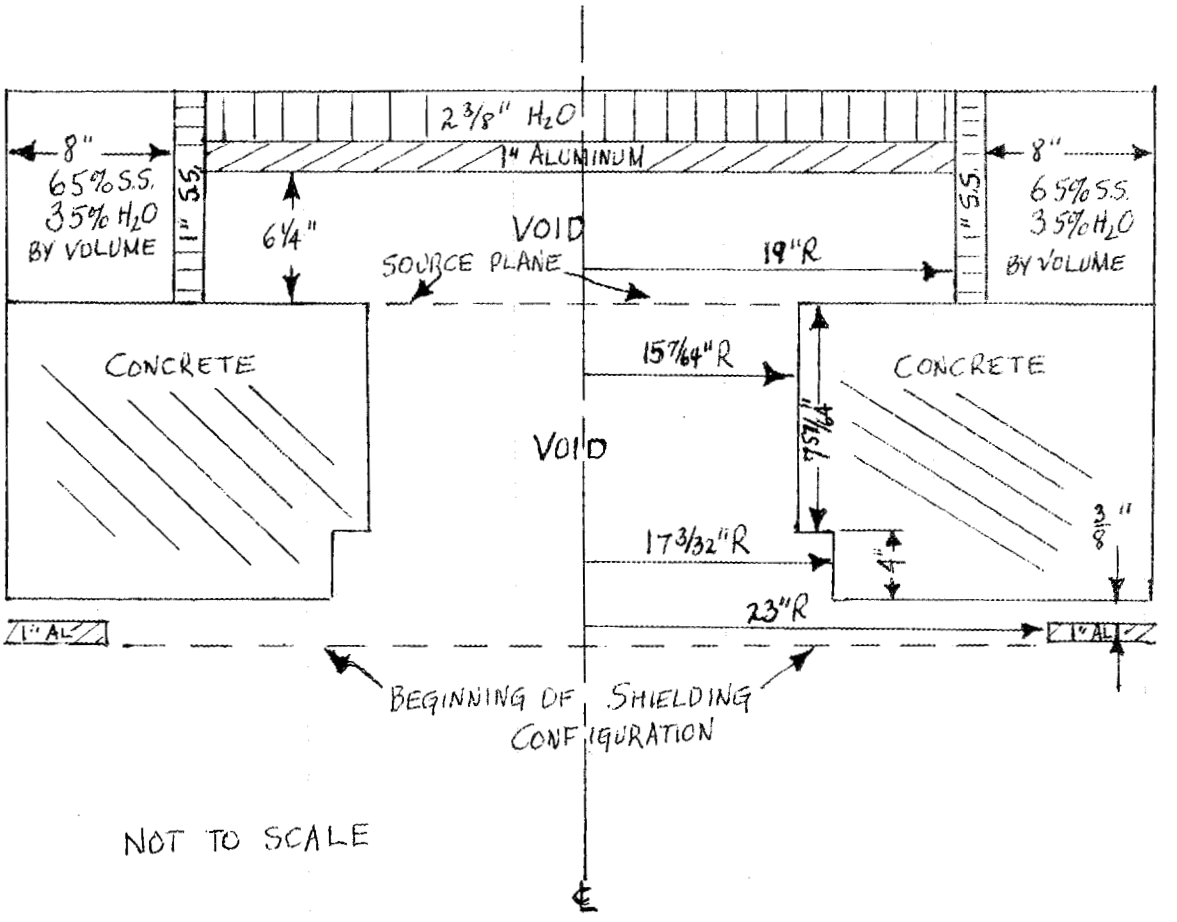

Fig. 2. Two-Dimensional Approximations to Figure 1 to Describe the Source and Collimator Geometry.

Table I. Angular Fluxes at the Surface of the Pressure Vessel: Source Terms for the Large Beam Collimator

Group	E_u	Flux (neutrons/cm^2/min/fission watt/unit weight) for $\cos\theta_n$ of							
		.0950124	.281603	.458017	.617876	.755404	.865631	.944574	.989401
1	14.92 MeV	1.82(2)*	6.03(2)	1.39(3)	4.37(3)	1.34(4)	2.26(4)	2.35(4)	2.31(4)
2	12.21	1.11(3)	3.38(3)	7.40(3)	2.21(4)	6.71(4)	1.16(5)	1.20(5)	1.20(5)
3	10.000	4.50(3)	1.35(4)	2.77(4)	7.87(4)	2.38(5)	4.10(5)	4.30(5)	4.32(5)
4	8.187	1.66(4)	4.58(4)	8.48(5)	2.11(5)	5.88(5)	1.01(6)	1.09(6)	1.11(6)
5	6.703	5.56(4)	1.39(5)	2.24(5)	4.73(5)	1.19(6)	2.00(6)	2.24(6)	2.33(6)
6	5.488	1.42(5)	3.29(5)	4.72(5)	8.63(5)	1.94(6)	3.15(6)	3.63(6)	3.83(6)
7	4.493	2.30(5)	5.02(5)	6.63(5)	1.07(6)	2.08(6)	3.32(6)	4.00(6)	4.35(6)
8	3.679	3.64(5)	7.76(5)	9.88(5)	1.48(6)	2.59(6)	3.96(6)	4.84(6)	5.30(6)
9	3.012	5.67(5)	1.16(6)	1.39(6)	1.98(6)	3.46(6)	5.21(6)	6.33(6)	6.89(6)
10	2.466	7.64(5)	1.56(6)	1.78(6)	2.35(6)	3.89(6)	5.69(6)	6.89(6)	7.53(6)
11	2.019	8.63(5)	1.68(6)	1.81(6)	2.26(6)	3.43(6)	4.81(6)	5.89(6)	6.47(6)
12	1.653	8.23(5)	1.59(6)	1.74(6)	2.13(6)	3.06(6)	4.17(6)	5.08(6)	5.59(6)
13	1.353	7.62(5)	1.43(6)	1.61(6)	1.96(6)	2.61(6)	3.38(6)	4.07(6)	4.46(6)
14	1.1080	7.96(5)	1.53(6)	1.61(6)	1.81(6)	2.28(6)	2.78(6)	3.28(6)	3.56(6)
15	0.9072	6.49(5)	1.16(6)	1.34(6)	1.63(6)	2.03(6)	2.52(6)	2.94(6)	3.21(6)
16	0.7427	7.32(5)	1.37(6)	1.50(6)	1.74(6)	2.15(6)	2.60(6)	3.02(6)	3.28(6)
17	0.6081	6.64(5)	1.19(6)	1.33(6)	1.53(6)	1.86(6)	2.21(6)	2.51(6)	2.70(6)
18	0.4978	4.68(5)	8.14(5)	9.04(5)	1.05(6)	1.19(6)	1.35(6)	1.48(6)	1.57(6)
19	0.4076	5.54(5)	1.06(6)	1.17(6)	1.31(6)	1.51(6)	1.71(6)	1.88(6)	1.97(6)
20	0.3337	3.67(5)	6.40(5)	7.48(5)	9.16(5)	1.07(6)	1.23(6)	1.36(6)	1.44(6)
21	0.2732	3.91(5)	7.73(5)	8.93(5)	1.02(6)	1.18(6)	1.32(6)	1.44(6)	1.53(6)
22	0.2237	3.29(5)	5.50(5)	6.30(5)	7.53(5)	8.58(5)	9.70(5)	1.06(6)	1.11(6)
23	0.1832	1.62(5)	2.49(5)	3.00(5)	3.88(5)	4.66(5)	5.47(5)	6.06(5)	6.44(5)
24	0.1500	5.25(5)	9.31(5)	1.02(6)	1.07(6)	1.14(6)	1.22(6)	1.27(6)	1.31(6)
25	0.12277	1.93(5)	3.15(5)	3.98(5)	5.39(5)	6.59(5)	7.70(5)	8.50(5)	8.97(5)
26	86.52 keV	6.76(5)	1.41(6)	1.61(6)	1.68(6)	1.85(6)	1.96(6)	2.07(6)	2.13(6)
27	52.48	1.53(5)	2.90(5)	3.78(5)	4.84(5)	5.53(5)	6.19(5)	6.61(5)	6.93(5)
28	40.86	7.81(4)	1.08(5)	1.27(5)	1.57(5)	1.85(5)	2.16(5)	2.38(5)	2.52(5)
29	31.83	3.36(5)	9.63(5)	1.07(6)	8.61(5)	9.93(5)	9.79(5)	1.03(6)	1.04(6)
30	24.79	6.99(4)	2.25(5)	4.51(5)	5.52(5)	5.78(5)	6.48(5)	6.66(5)	6.94(5)
31	19.30	7.29(4)	2.04(5)	3.86(5)	4.90(5)	5.21(5)	5.87(5)	6.09(5)	6.31(5)
32	15.03	3.08(5)	7.70(5)	1.26(6)	1.60(6)	1.75(6)	1.95(6)	2.04(6)	2.11(6)
33	7.102	2.23(5)	5.17(5)	7.69(5)	9.80(5)	1.09(6)	1.21(6)	1.28(6)	1.33(6)
34	4.307	1.02(5)	2.46(5)	3.77(5)	4.79(5)	5.33(5)	5.96(5)	6.29(5)	6.55(5)
35	3.355	9.94(4)	2.38(5)	3.64(5)	4.63(5)	5.19(5)	5.80(5)	6.13(5)	6.40(5)

36	2.613	1.00(5)	2.37(5)	3.61(5)	4.59(5)	5.17(5)	5.78(5)	6.10(5)	6.38(5)
37	2.035	1.01(5)	2.37(5)	3.60(5)	4.56(5)	5.15(5)	5.77(5)	6.09(5)	6.36(5)
38	1.585	9.93(4)	2.34(5)	3.51(5)	4.49(5)	5.07(5)	5.66(5)	6.02(5)	6.29(5)
39	1.2341	9.79(4)	2.30(5)	3.46(5)	4.42(5)	5.00(5)	5.63(5)	5.95(5)	6.22(5)
40	961.1 eV	2.91(5)	6.83(5)	1.03(6)	1.32(6)	1.50(6)	1.67(6)	1.78(6)	1.85(6)
41	454.0	2.91(5)	6.82(5)	1.02(6)	1.30(6)	1.48(6)	1.67(6)	1.78(6)	1.85(6)
42	214.5	2.88(5)	6.75(5)	1.01(6)	1.29(6)	1.47(6)	1.65(6)	1.78(6)	1.83(6)
43	101.3	2.88(5)	6.78(5)	1.01(6)	1.29(6)	1.48(6)	1.67(6)	1.78(6)	1.85(6)
44	47.85	2.91(5)	6.82(5)	1.01(6)	1.30(6)	1.50(6)	1.68(6)	1.81(6)	1.86(6)
45	22.60	2.91(5)	6.83(5)	1.01(6)	1.30(6)	1.50(6)	1.68(6)	1.81(6)	1.88(6)
46	10.677	3.54(5)	8.29(5)	1.23(6)	1.58(6)	1.83(6)	2.06(6)	2.20(6)	2.30(6)
47	5.043	3.51(5)	8.18(5)	1.22(6)	1.55(6)	1.82(6)	2.06(6)	2.20(6)	2.28(6)
48	2.382	4.19(5)	9.80(5)	1.46(6)	1.89(6)	2.17(6)	2.45(6)	2.62(6)	2.73(6)
49	1.125	8.34(5)	1.96(6)	2.93(6)	3.79(6)	4.37(6)	4.93(6)	5.26(6)	5.50(6)
50	0.4140	1.40(6)	3.26(6)	4.93(6)	6.45(6)	7.42(6)	8.40(6)	9.02(6)	9.37(6)
51	0.1000	9.43(6)	2.18(7)	3.42(7)	4.60(7)	5.21(7)	5.92(7)	6.25(7)	6.54(7)

*Read as 2.30×10^4.

APPENDIX

```
      DIMENSIØN CUR(51,8),AETA(8),ETA(15),AMU(15,10),NØMU(15),INDX(15),
     1FDET(51,100),FLTAPE(266000)
      DØ 2 IE=1,51
    2 READ(5,130)(CUR(IE,IT),IT=1,8)
      READ(5,170)(AETA(IT),IT=1,8)
      DØ 1 I=1,8
      DØ 1 IE=1,51
    1 CUR(IE,I)=CUR(IE,I)*AETA(I)
      READ(5,170)(ETA(I),I=1,15)
      READ(5,110)(NØMU(I),I=1,15)
      DØ 3 I=1,15
      NL=NØMU(I)
    3 READ(5,170)(AMU(I,J),J=1,NL)
      READ(5,110)(INDX(I),I=1,15)
  110 FØRMAT(14I5)
  130 FØRMAT(8E9.2)
  170 FORMAT(7E10.5)
      DØ 20 I=1,266000
   20 FLTAPE(I)=0.
      DØ 100 ID=1,19
      DØ 15 IA=1,100
      DØ 15 IE=1,51
```

```
15 FDET(IE,IA)=0.
   FID=FLØAT(ID)
   XD=1.27+2.54*(FID-1.)
   DØ 51 I=1,15
   FETA=ETA(I)
   JLEVEL=NØMU(I)
   DØ 40 J=1,JLEVEL
   IA=J+INDX(I)
   FMU=AMU(I,J)
   D=FMU*XD+FETA*55.514
   DISC=-722.03069-XD*XD+D*D
   IF(DISC)40,40,12
 12 A=D-SØRT(DISC)
   CØSN=(722.03069+XD*XD-A*A)/(97.155*A)
   IF(CØSN)40,40,13
 13 DØ 60 IC=1,8
   IF(CØSN-AETA(IC))65,65,60
 60 CØNTINUE
   IC=9
 65 IF(IC-1)66,66,67
 66 FRAC=(AETA(1)*AETA(1)-CØSN*CØSN)/(AETA(1)*AETA(1))
   GØ TØ 70
 67 IF(IC-9)69,68,68
 68 FRAC1=(AETA(8)*AETA(8)-CØSN*CØSN)/(AETA(8)*AETA(8)-AETA(7)
  1*AETA(7))
   FRAC2=(CØSN*CØSN-AETA(7)*AETA(7))/(AETA(8)*AETA(8)-AETA(7)
```

```
  1*AETA(7))
   GØ TØ 70
69 FRAC=(AETA(IC)*AETA(IC)-CØSN*CØSN)/(AETA(IC)*AETA(IC)-AETA(IC-1)
  1*AETA(IC-1))
70 DØ 76 IE=1,51
   IF(IC-1)71,71,72
71 ANGJ=CUR(IE,1)*(1.-FRAC)
   GØ TØ 75
72 IF(IC-9)74,73,73
73 ANGJ=CUR(IE,7)*FRAC1+CUR(IE,8)*FRAC2
   GØ TØ 75
74 ANGJ=CUR(IE,IC)*(1.-FRAC)+CUR(IE,IC-1)*FRAC
75 FDET(IE,IA)=FDET(IE,IA)+ANGJ/FETA
76 CØNTINUE
40 CØNTINUE
51 CØNTINUE
   DØ 25  IA=1,100
   DØ 25 IE=1,51
   IX=5200*(IE-1)+100*(ID-1)+IA
25 FLTAPE(IX)=FDET(IE,IA)
100 CØNTINUE
   DØ 80 IE=1,51
   IU=5200*IE
   IL=IU-5199
80 WRITE(1)(FLTAPE(I),I=IL,IU)
   WRITE(6,90)(FLTAPE(I),I=1,5200)
```

```
90 FØRMAT(1HO,1P12E9.2)
   STØP
   END
```

Note the following input and conventions:

CUR(IE,IT) = data in Table I, each IE corresponds to the row as printed

AETA(IT) = positive part of S_{16} ANISN quadrature angles, in order presented in Table I

ETA(I) = forward values of $|\eta|$ of S_{100} DØT quadrature angular set (see next section of appendix)

NØMU(I) = number of μ levels for each value of $|\eta|$, and consists of 11 values of 2 followed by 4, 6, 8, and 10

AMU(I,J) = NØMU(I) values of μ for each value of $|\eta|$ (see next section of appendix)

INDX(I) = index for locations of angles having zero weight for forward part of S_{100} set = 1, 4, 7, 10, 13, 16, 19, 22, 25, 28, 31, 34, 39, 46, 55

The DØT geometry is assumed to be set up with the direction of positive Z upward and the forward values of η negative. There are 52 radial intervals, in which the source is non-zero over the first 19.

Table A1. Forward Values of $|\eta|$ and μ having Associated Non-Zero Weights for the S_{100} Asymmetrical Quadrature Set. Input to the Transformation Code.

I	ETA(I)	J	AMU(I,J)	I	ETA(I)	J	AMU(I,J)
1	.99963	1	-.016595	13	.67940	1	-.67942
		2	.016595			2	-.43340
2	.99836	1	-.037554			3	-.14888
		2	.037554			4	.14888
3	.99598	1	-.058760			5	.43340
		2	.058760			6	.67942
4	.99254	1	-.0799769	14	.43339	7	-.86507
		2	.0799769			2	-.67941
5	.98805	1	-.10111			3	-.43340
		2	.10111			4	-.14887
6	.98251	1	-.12215			5	.14887
		2	.12215			6	.43340
7	.97593	1	-.14306			7	.67941
		2	.14306			8	.86507
8	.96832	1	-.16381	15	.14887	1	-.97391
		2	.16381			2	-.86506
9	.95968	1	-.18439			3	-.67941
		2	.18439			4	-.43340
10	.95003	1	-.20477			5	-.14887
		2	.20477			6	.14887
11	.93937	1	-.22494			7	.43340
		2	.22494			8	.67941
12	.86506	1	-.43340			9	.86506
		2	-.14888			10	.97391
		3	.14888				
		4	.43340				

This page has been left blank intentionally.

Table A2. Angular Fluxes in Neutrons/cm^2/min/fission watt/unit Weight for Group 1 on the Disc Plane. Output from the Transformation Code and Source to be used in DOT.

ANGLE/RAD	1.27	3.81	6.35	8.89	11.43	13.97	16.51	19.05	21.59	24.13
1	0	0	0	0	0	0	0	0	0	
2	2.30(4)*	2.30(4)	2.29(4)	2.27(4)	2.26(4)	2.23(4)	2.18(4)	2.11(4)	2.02(4)	1.88(4)
3	2.31(4)	2.30(4)	2.30(4)	2.29(4)	2.27(4)	2.25(4)	2.23(4)	2.16(4)	2.09(4)	2.00(4)
4	0	0	0	0	0	0	0	0	0	0
5	2.30(4)	2.30(4)	2.28(4)	2.27(4)	2.25(4)	2.22(4)	2.15(4)	2.07(4)	1.98(4)	1.74(4)
6	2.31(4)	2.31(4)	2.30(4)	2.29(4)	2.28(4)	2.26(4)	2.24(4)	2.20(4)	2.12(4)	2.04(4)
7	0	0	0	0	0	0	0	0	0	0
8	2.30(4)	2.29(4)	2.28(4)	2.26(4)	2.24(4)	2.19(4)	2.11(4)	2.03(4)	1.88(4)	1.58(4)
9	2.31(4)	2.31(4)	2.31(4)	2.30(4)	2.29(4)	2.27(4)	2.25(4)	2.23(4)	2.16(4)	2.08(4)
10	0	0	0	0	0	0	0	0	0	0
11	2.30(4)	2.29(4)	2.28(4)	2.26(4)	2.22(4)	2.15(4)	2.08(4)	1.99(4)	1.73(4)	1.42(4)
12	2.31(4)	2.31(4)	2.31(4)	2.31(4)	2.30(4)	2.28(4)	2.27(4)	2.24(4)	2.19(4)	2.11(4)
13	0	0	0	0	0	0	0	0	0	0
14	2.30(4)	2.29(4)	2.27(4)	2.25(4)	2.19(4)	2.12(4)	2.03(4)	1.86(4)	1.57(4)	1.24(4)
15	2.31(4)	2.32(4)	2.32(4)	2.32(4)	2.31(4)	2.30(4)	2.28(4)	2.26(4)	2.22(4)	2.15(4)
16	0	0	0	0	0	0	0	0	0	0
17	2.31(4)	2.29(4)	2.27(4)	2.22(4)	2.16(4)	2.08(4)	1.98(4)	1.70(4)	1.39(4)	1.06(4)
18	2.32(4)	2.32(4)	2.33(4)	2.32(4)	2.32(4)	2.31(4)	2.30(4)	2.28(4)	2.24(4)	2.18(4)
19	0	0	0	0	0	0	0	0	0	0
20	2.31(4)	2.29(4)	2.25(4)	2.19(4)	2.12(4)	2.04(4)	1.83(4)	1.53(4)	1.21(4)	9.04(3)
21	2.32(4)	2.33(4)	2.33(4)	2.33(4)	2.33(4)	2.32(4)	2.31(4)	2.29(4)	2.27(4)	2.21(4)
22	0	0	0	0	0	0	0	0	0	0
23	2.31(4)	2.28(4)	2.22(4)	2.16(4)	2.08(4)	1.94(4)	1.66(4)	1.35(4)	1.02(4)	7.51(3)
24	2.32(4)	2.33(4)	2.34(4)	2.34(4)	2.34(4)	2.34(4)	2.32(4)	2.31(4)	2.29(4)	2.23(4)
25	0	0	0	0	0	0	0	0	0	0
26	2.30(4)	2.25(4)	2.19(4)	2.12(4)	2.03(4)	1.77(4)	1.48(4)	1.16(4)	8.72(3)	5.91(3)
27	2.33(4)	2.34(4)	2.35(4)	2.35(4)	2.35(4)	2.35(4)	2.34(4)	2.33(4)	2.30(4)	2.25(4)
28	0	0	0	0	0	0	0	0	0	0
29	2.28(4)	2.22(4)	2.16(4)	2.08(4)	1.87(4)	1.59(4)	1.29(4)	9.84(3)	7.14(3)	4.23(3)

30	2.32(4)	2.35(4)	2.36(4)	2.36(4)	2.37(4)	2.36(4)	2.36(4)	2.35(4)	2.32(4)	2.27(4)
31	0	0	0	0	0	0	0	0	0	0
32	2.25(4)	2.19(4)	2.12(4)	1.95(4)	1.69(4)	1.41(4)	1.09(4)	8.28(3)	5.49(3)	2.75(3)
33	2.30(4)	2.34(4)	2.37(4)	2.37(4)	2.38(4)	2.38(4)	2.37(4)	2.36(4)	2.33(4)	2.29(4)
34	0	0	0	0	0	0	0	0	0	0
35	1.65(4)	1.34(4)	1.05(4)	7.91(3)	5.07(3)	2.79(3)	1.80(3)	7.45(2)	4.06(2)	1.11(2)
36	1.73(4)	1.61(4)	1.45(4)	1.26(4)	1.07(4)	8.75(3)	6.59(3)	4.20(3)	2.64(3)	1.76(3)
37	1.83(4)	1.89(4)	1.92(4)	1.92(4)	1.88(4)	1.81(4)	1.71(4)	1.57(4)	1.40(4)	1.20(4)
38	1.92(4)	2.17(4)	2.31(4)	2.37(4)	2.43(4)	2.48(4)	2.52(4)	2.55(4)	2.57(4)	2.57(4)
39	0	0	0	0	0	0	0	0	0	0
40	1.98(3)	9.55(2)	6.21(2)	2.84(2)	5.67(1)	0	0	0	0	0
41	2.15(3)	1.45(3)	8.60(2)	6.04(2)	3.25(2)	1.12(2)	0	0	0	0
42	2.36(3)	2.05(3)	1.65(3)	1.15(3)	8.25(2)	6.20(2)	3.87(2)	1.75(2)	2.65(0)	0
43	2.57(3)	2.69(3)	2.71(3)	2.64(3)	2.48(3)	2.22(3)	1.87(3)	1.42(3)	9.20(2)	7.30(2)
44	2.77(3)	3.32(3)	3.78(3)	4.61(3)	5.62(3)	6.37(3)	6.86(3)	7.10(3)	7.08(3)	6.80(3)
45	2.95(3)	3.88(3)	6.50(3)	9.18(3)	1.17(4)	1.40(4)	1.66(4)	1.93(4)	2.18(4)	2.40(4)
46-52	0	0	0	0	0	0	0	0	0	0
53	0	0	8.53(1)	2.17(2)	3.35(2)	4.67(2)	6.11(2)	7.32(2)	8.28(2)	9.00(2)
54	0	2.20(1)	2.30(2)	4.61(2)	7.86(2)	1.10(3)	1.40(3)	2.21(3)	3.15(3)	4.05(3)
55-100	0	0	0	0	0	0	0	0	0	0

*Read as 2.30×10^4.

Continuation

Table A2. Angular Fluxes in Neutrons/cm^2/min/fission watt/unit Weight for Group 1 on the Disc Plane. Output from the Transformation Code and Source to be used in DOT.

ANGLE/RAD	26.67	29.21	31.75	34.29	36.83	39.37	41.91	44.45	46.99	>46.99
1	0	0	0	0	0	0	0	0	0	0
2	1.58(4)	1.25(4)	9.20(3)	6.33(3)	3.25(3)	1.86(3)	7.88(2)	3.42(2)	5.64(1)	0
3	1.80(4)	1.49(4)	1.15(4)	8.44(3)	5.51(3)	2.60(3)	1.57(3)	5.91(2)	2.45(2)	0
4	0	0	0	0	0	0	0	0	0	0
5	1.42(4)	1.08(4)	7.87(3)	4.90(3)	2.40(3)	1.37(3)	5.26(2)	1.77(2)	0	0
6	1.92(4)	1.63(4)	1.30(4)	9.66(3)	6.83(3)	3.78(3)	2.04(3)	9.77(2)	4.03(2)	0
7	0	0	0	0	0	0	0	0	0	0
8	1.26(4)	9.29(3)	6.44(3)	3.37(3)	1.91(3)	8.41(2)	3.61(2)	6.90(1)	0	0
9	1.99(4)	1.75(4)	1.44(4)	1.10(4)	8.08(3)	5.14(3)	2.49(3)	1.46(3)	5.56(2)	0
10	0	0	0	0	0	0	0	0	0	0
11	1.08(4)	7.88(3)	4.93(3)	2.43(3)	1.39(3)	5.38(2)	1.90(2)	0	0	0
12	2.03(4)	1.87(4)	1.57(4)	1.25(4)	9.26(3)	6.41(3)	3.34(3)	1.91(3)	8.42(2)	0
13	0	0	0	0	0	0	0	0	0	0
14	9.23(3)	6.39(3)	3.33(3)	1.92(3)	8.53(2)	3.69(2)	7.51(1)	0	0	0
15	2.07(4)	1.98(4)	1.69(4)	1.38(4)	1.04(4)	7.59(3)	4.62(3)	2.34(3)	1.30(3)	0
16	0	0	0	0	0	0	0	0	0	0
17	7.76(3)	4.82(3)	2.42(3)	1.39(3)	5.42(2)	1.95(2)	0	0	0	0
18	2.10(4)	2.02(4)	1.80(4)	1.50(4)	1.17(4)	8.67(3)	5.80(3)	2.74(3)	1.73(3)	0
19	0	0	0	0	0	0	0	0	0	0
20	6.21(3)	3.17(3)	1.89(3)	8.34(2)	3.71(2)	7.74(1)	0	0	0	0
21	2.14(4)	2.06(4)	1.89(4)	1.60(4)	1.29(4)	9.66(3)	6.88(3)	3.89(3)	2.13(3)	0
22	0	0	0	0	0	0	0	0	0	0
23	4.59(3)	2.38(3)	1.35(3)	5.40(2)	1.94(2)	0	0	0	0	0
24	2.17(4)	2.09(4)	1.97(4)	1.70(4)	1.39(4)	1.06(4)	7.86(3)	4.97(3)	2.50(3)	0
25	0	0	0	0	0	0	0	0	0	0
26	2.89(3)	1.84(3)	7.89(2)	3.66(2)	7.65(1)	0	0	0	0	0
27	2.19(4)	2.12(4)	2.04(4)	1.77(4)	1.48(4)	1.16(4)	8.74(3)	5.93(3)	2.91(3)	0
28	0	0	0	0	0	0	0	0	0	0
29	2.31(3)	1.29(3)	5.31(2)	1.87(2)	0	0	0	0	0	0

30	2.21(4)	2.15(4)	2.07(4)	1.84(4)	1.56(4)	1.25(4)	9.51(3)	6.79(3)	3.86(3)	0
31	0	0	0	0	0	0	0	0	0	0
32	1.77(3)	7.16(2)	3.56(2)	7.26(1)	0	0	0	0	0	0
33	2.23(4)	2.17(4)	2.10(4)	1.89(4)	1.62(4)	1.32(4)	1.02(4)	7.54(3)	4.69(3)	0
34-35	0	0	0	0	0	0	0	0	0	0
36	8.08(2)	4.51(2)	1.51(2)	0	0	0	0	0	0	0
37	1.02(4)	8.25(3)	6.04(3)	3.58(3)	2.44(3)	1.54(3)	6.85(2)	3.73(2)	1.00(2)	0
38	2.57(4)	2.57(4)	2.55(4)	2.52(4)	2.49 (4)	2.44(4)	2.38(4)	2.32(4)	2.21(4)	0
39-42	0	0	0	0	0	0	0	0	0	0
43	5.12(2)	2.66(2)	9.32(1)	0	0	0	0	0	0	0
44	6.27(3)	5.48(3)	4.43(3)	3.72(3)	3.24(3)	2.69(3)	2.05(3)	1.34(3)	8.22(2)	0
45	2.60(4)	2.78(4)	2.90(4)	2.95(4)	2.99(4)	3.02(4)	3.04(4)	3.05(4)	3.06(4)	0
46-52	0	0	0	0	0	0	0	0	0	0
53	9.47(2)	9.71(2)	9.69(2)	9.44(2)	8.94(2)	8.20(2)	7.22(2)	5.99(2)	4.52(2)	0
54	4.90(3)	5.72(3)	7.14(3)	9.58(3)	1.19(4)	1.41(4)	1.62(4)	1.81(4)	1.99(4)	0
55-100	0	0	0	0	0	0	0	0	0	0

Table A3. DOT Output Disc Source Summary for Groups 1-49, in Neutrons/min/fission watt

Group	Fixed Source	Group	Fixed Source
1	1.14424(7)	26	1.45171(9)
2	5.83158(7)	27	4.32258(8)
3	2.07651(8)	28	1.49226(8)
4	5.21222(8)	29	7.68712(8)
5	1.06625(9)	30	4.55593(8)
6	1.73712(9)	31	4.09954(8)
7	1.91209(9)	32	1.36463(9)
8	2.36146(9)	33	8.50067(8)
9	3.12387(9)	34	4.16490(8)
10	3.48332(9)	35	4.04836(8)
11	3.05339(9)	36	4.02802(8)
12	2.69831(9)	37	4.01548(8)
13	2.25118(9)	38	3.95059(8)
14	1.92055(9)	39	3.90654(8)
15	1.71017(9)	40	1.16313(9)
16	1.79311(9)	41	1.15849(9)
17	1.53232(9)	42	1.15120(9)
18	9.61185(8)	43	1.15613(9)
19	1.21824(9)	44	1.16751(9)
20	8.59587(8)	45	1.16720(9)
21	9.38762(8)	46	1.42494(9)
22	6.86375(8)	47	1.41794(9)
23	3.74450(8)	48	1.69494(9)
24	9.05490(8)	49	3.40779(9)
25	5.22314(8)	1-49	5.71109(10)

ORNL-TM-5183
UC-79d - Liquid
Metal Fast Breeder
Reactor Physics

INTERNAL DISTRIBUTION

1-3. L. S. Abbott
4. D. E. Bartine
5. R. L. Childs
6. C. E. Clifford
7. M. B. Emmett
8. W. W. Engle, Jr.
9. R. M. Freestone, Jr.
10. H. Goldstein
11. W. O. Harms
12. R. E. Maerker
13. F. C. Maienschein
14. F. J. Muckenthaler
15. F. R. Mynatt
16. E. M. Oblow
17. C. O. Slater
18. P. N. Stevens
19. D. K. Trubey
20. L. R. Williams
21. M. L. Williams
22. A. Zucker
23. P. F. Fox (consultant)
24. W. W. Havens, Jr. (consultant)
25. A. F. Henry (consultant)
26-27. Central Research Library
28. ORNL Y-12 Technical Library Document Reference Section
29-30. Laboratory Records
31. Laboratory Records ORNL RC
32. ORNL Patent Office
33. RSIC

EXTERNAL DISTRIBUTION

33-34. USERDA Division of Reactor Research and Development, Washington, DC 20545: Director
35. USERDA Oak Ridge Operations, Reactor Division, P. O. Box E, Oak Ridge, TN 37830: Director
36. USERDA Oak Ridge Operations, Research and Technical Support Division, P. O. Box E, Oak Ridge, TN 37830: Director
37-240. For distribution as shown in TID-4500 Distribution Category, UC-79d, Liquid Metal Fast Breeder Reactor Physics